

Optimizing an Observing Plan for *Roman* Astrometry of Terra Hunting Stars to Determine P(Jupiter | Earth)

DANIEL A. YAHALOMI ¹, DAVID N. SPERGER ², AND RUTH ANGUS ^{3,2,1}

¹*Department of Astronomy, Columbia University, 550 W 120th St., New York NY 10027, USA*

²*Center for Computational Astrophysics, Flatiron Institute, 162 5th Avenue, New York, NY 10010, USA*

³*American Museum of Natural History, Central Park West, Manhattan, NY, USA*

ABSTRACT

Earth-mass planets on year-long orbits and gas giants on decade-long orbits lie at the edge of current detection limits. The *Nancy Grace Roman Space Telescope*, scheduled to launch in late 2025, will be capable of precision astrometry using its wide field imager. For bright stars, *Roman* may be able to achieve astrometric accuracy of 1-10 μ as. By combining measurements from a *Roman* astrometry observing program with Gaia data we can increase the baseline of astrometric observations in order to recover planets on wide, Jupiter-like orbits. The Terra Hunting Experiment (THE), starting in 2022, will take nightly radial velocity (RV) observations of at least 40 bright G and K dwarfs for 10 years, in search of planets that are Earth-like in mass and temperature. Together, *Roman* and THE may be capable of detecting both Earth-analogues and Jupiter-analogues. In order to design and optimize an observing strategy for *Roman* astrometry, we simulate a set of possible planetary signals both in single and multi-planet systems, based on planetary architecture and stability models. Jupiter has played a significant dynamical role in our own Solar system, and the occurrence rate of outer Jovian planets in systems with terrestrial planets could inform planet formation and dynamical evolution models. We describe an observing plan that could provide estimates on P(Jupiter | Earth), the probability that a star has a Jupiter analogue, given that it has an Earth analogue.

1. INTRODUCTION

The detection and study of extrasolar planets (exoplanets) has a long history of exciting and surprising discoveries. Astronomers have detected worlds vastly different than those in our own solar system : ‘zombie’ planets orbiting a pulsar (Wolszczan & Frail 1992), so called hot Jupiters or gas giants orbiting a star at shorter than 10 day periods (Latham et al. 1989; Mayor & Queloz 1995), planets orbiting main sequence binary star systems (Correia et al. 2005), (...other exotic planet types) – nice but not necessary. However, despite all this progress in the field of exoplanets, astronomers have yet to detect true Solar system analogs. This has been driven by observational detection limits, as both Earth-mass objects on year-long orbits and gas-giant planets on 10 year (Jupiter-like) or longer orbits lie outside of current telescope capabilities. Figure 1 shows the current exoplanet detections as well as the Earth

and Jupiter in mass vs. period space. Always explain a figure in the text and hammer the point home. What point is figure 1 illustrating and how?

In the coming decade, with radial velocity surveys designed for the purpose of Earth-twin detection (Hall et al. 2018) and with astrometric observations from space missions like *Gaia*, which will release astrometry in data release 4 (DR4) (Gaia Collaboration et al. 2016) and *The Nancy Grace Roman*, set to launch in late 2025 (Spergel et al. 2015), there is promise in the detection of Solar System analogs. While it has been demonstrated that *Roman* will contribute heavily to exoplanet science via the microlensing method (Penny et al. 2019; Johnson et al. 2020), it will also be capable of high precision astrometric exoplanet detection (WFIRST Astrometry Working Group et al. 2019). Astrometric observations complement radial velocity surveys targeting Earth-analogs in that (1) astrometric measurements can break the mass-inclination degeneracy inherent in radial velocity observations, (2) astrometric measurements, which are more sensitive to longer periods, complement RV observations, which are more sensitive to shorter periods, and (3) astrometric observation could

allow us to marginalize over stellar noise in the RV data as astrometry is less sensitive to stellar noise than the Doppler method. **Great!** The detection capabilities of astrometric surveys drop very steeply when the period of the orbit extends past the duration of the astrometric observations (Casertano et al. 2008). Thus, in targeting planets on long orbits with astrometry, combining observations from *Gaia* and *Roman* will be critical in extending the period baseline for detection capabilities.

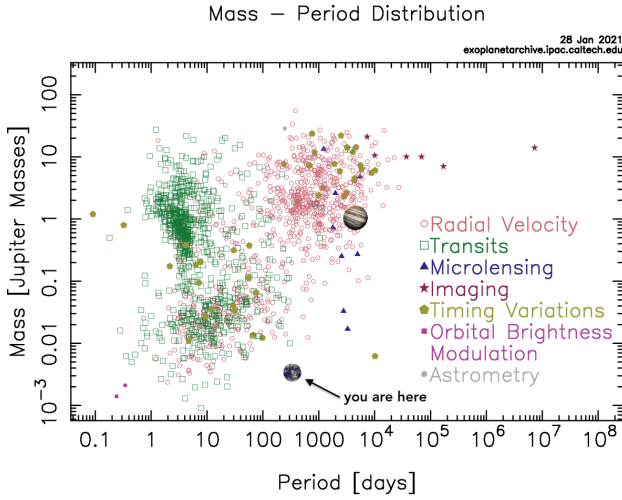


Figure 1. Mass vs. orbital period of confirmed exoplanets and the method of detection. Earth and Jupiter are also plotted. The paucity of planets at low masses and long periods reflects the limitations of our observational techniques rather than true exoplanet demographics.. Demographics figure generated with tools from exoplanetarchive.ipac.caltech.edu.

The formation and migration of gas giant planets and the interactions between gas giants in our Solar System have played a critical role in the characteristics of the planets in our Solar System (Tsiganis et al. 2005; Morbidelli et al. 2005; Gomes et al. 2005; Walsh et al. 2011; Batygin & Laughlin 2015). Further, Jupiter may have played a crucial role in Earth’s habitability, in that it (1) helps stabilize Earth’s orbit and thus climate and (2) it shields Earth from possibly devastating impacts (Raymond et al. 2004) **would like another resource here**. As the Earth is the only presently known habitable planet, it is natural to search for Earth-twins in pursuit of habitable planets. Further, if Jupiter (and Saturn) have played such an important role both in the formation, stability, and habitability of Earth, it is also of interest to search for Earth-analogues with external gas giant planets. Thus, in order to better understand the demographics of Earth-analogues, an important question to investigate is the percentage of Earth-analogues that also have Jupiter-like (or Saturn-like) companions. **Very well explained.**

In this paper, we present an observing strategy with *Roman* astrometry, capable of detecting both Earth-analogues and Jupiter-analogues around Terra Hunting Stars. By combining observations from the Terra Hunting Doppler survey with *Gaia* and *Roman* astrometry, we can investigate the probability that a Solar-type star has an orbiting Jupiter-like planet, given that the Solar-type star has an orbiting Earth-like planet ($P(\text{Jupiter}|\text{Earth})$). Specifically, in this proposed *Roman* observing strategy, we will obtain follow-up astrometric observations of stars that show radial velocity signals consistent with an Earth-analogue via the Terra Hunting Experiment.

In combination with exoplanet demographic models, one could then infer, using Bayes theory, the probability that a Solar-type star has an orbiting Earth-like planet, given that the star has an orbiting Jupiter-like planet ($P(\text{Earth}|\text{Jupiter})$), by using the Equation 1.

$$P(\text{Earth}|\text{Jupiter}) = \frac{P(\text{Jupiter}|\text{Earth}) P(\text{Earth})}{P(\text{Jupiter})} \quad (1)$$

This version of the equation has the inherent benefit, in that it is easier to detect Jupiter analogues, as they are so much more massive than Earth-like planets, and thus have a larger gravitational effect on their host star. However, this version of the equation has the downside in that the model would be built on assumptions of $P(\text{Earth})$ and $P(\text{Jupiter})$.

To date, similar studies have been conducted for super-Earths and cold-Jupiters (Zhu & Wu 2018; Masuda et al. 2020) as well as for hot-Jupiters and cold-Jupiters (Knutson et al. 2014). Zhu & Wu (2018) investigated the relations between inner (< 1 AU) super-Earths and outer (> 1 AU) cold-Jupiters and determined $P(\text{cold-Jupiter}|\text{super-Earth}) \sim 30\%$. By comparing this value with results from Cumming et al. (2008), which predicts that 10% of Sun-like stars should have at least one cold-Jupiter, they determined that cold-Jupiters appear three times more often around super-Earth hosts than around Sun-like stars. Finally, by arguing that $P(\text{super-Earth}) = 30\%$ and using a version of Bayes theorem as shown in Equation 1, Zhu & Wu (2018) argued that $P(\text{super-Earth}|\text{cold-Jupiter}) \sim 90\%$. Subsequently, Masuda et al. (2020) showed that stellar systems with super-Earths and cold-Jupiters tend to be coplanar, but not quite as coplanar as the Solar System. Due to this and the strong association between the fraction of Sun-like stars that have both a cold-Jupiter and a super-Earth, they suggest that this provides a “clue” about the formation and evolution of these systems. Knutson et al. (2014) conducted a radial velocity study in search for long-period companions to

inner hot-Jupiters and found that in their sample of 51 systems, $51\% \pm 10\%$ of the systems had outer companions with masses between $1\text{--}13 M_{\text{Jup}}$ and orbital semi-major axes between $1\text{--}20$ AU. [Great review! Perhaps add a take-home statement here and frame a question that you would like to answer with Roman & THE?](#)

2. BACKGROUND, MISSIONS, AND EQUATIONS

[I suggest making mission backgrounds part of the introduction and moving equations to the methods section.](#)

2.1. Nancy Grace Roman Space Telescope

The *Nancy Grace Roman Space Telescope* is set to launch in 2025. *Roman* will be used to investigate many interesting and important topics in astronomy, such as studies of dark energy and dark matter, exoplanet detection and imaging, and a wide range of infrared astrometry. *Roman* will have a 2.4m primary lens, which is the same size as the *Hubble Space Telescope*, but a viewing window 100 times larger than *Hubble*. *Roman* will have no proprietary time and all observing time will be competed via external proposals. *Roman* has a five-year primary mission length.

As previously mentioned, *Roman* is expected to detect thousands of exoplanet microlensing events, which will be crucial in expanding the baseline of period sensitivity in exoplanet detection and improving our understanding of long period exoplanets ([Penny et al. 2019](#); [Johnson et al. 2020](#)). However, the microlensing method only provides for a single observation of a planetary system. *Roman* will also be capable of high precision astrometry and will provide at least a factor of three improvement over the current state of the art astrometric observations in this wavelength range. Further, *Roman* astrometry of bright nearby stars (< 10 pc) could detect Earth-mass exoplanets in some cases in the habitable zone, as well as more distant planets with periods up to >10 years by adding earlier astrometric observations from *Gaia* ([citations](#)). It is estimated that *Roman* will be capable of astrometric precision of $\sim 1\text{--}10 \mu\text{as}$ ([WFIRST Astrometry Working Group et al. 2019](#)).

As the stars we would like to observe are very bright, exoplanet astrometry with *Roman* can be pursued using two different methods, in order to avoid saturation:

1. **Diffraction Spike Method:** In the diffraction spike method, observations are centered on the detector's diffraction spike. This is possible as *Roman* uses H4RG detectors rather than CCDs, in which pixels bleed into nearby pixels when saturated. Measurement accuracy with this method will likely be limited by systematics, and so it is

ideal to take multiple observations of a system to reduce uncertainties ([WFIRST Astrometry Working Group et al. 2019](#)). [Melchior et al. \(2018\)](#) investigated the capabilities of a *Roman* dedicated guest observing plan using the diffraction spike method for detection of Earth-mass exoplanets. In the paper, they argued that *Roman* astrometry using the diffraction spike method could obtain $10 \mu\text{as}$ astrometric observations with a single 100s exposure for a $R=6$ or a $J=5$ star – precise enough to detect Earth-mass exoplanets on ≥ 1 year orbits around stars within a few pc.

2. **Spatial Scanning Method:** In the spatial scanning method, as the name suggests, the telescope is slowly slewed in a specific direction during the observation. This creates spatial tracks for the brighter stars and allows for the observation of reference stars in the same field. In so doing, this observational technique avoids saturation by spreading the signal over hundreds, or even thousands, of pixels – and thus allows for orders of magnitude of more photons. Subsequent spacial scans in two perpendicular directions allows for three-dimensional high precision observations. Similarly to the diffraction spike method, measurement accuracy with spatial scanning will likely be limited by systematics, and so it is ideal to take multiple observations of a system to reduce uncertainties ([WFIRST Astrometry Working Group et al. 2019](#)). This method has been applied to *Hubble* observations, in observing bright Cepheids with astrometric precision of $20\text{--}40 \mu\text{as}$ ([Riess et al. 2014](#)). [Very clear!](#)

2.2. Terra Hunting Experiment

The HARPS3 will be a fibre fed, high resolution, high stability, echelle spectrograph. The HARPS3 instrument will be installed on the 2.5m Isaac Newton Telescope in La Palma in the Canary Islands ([Thompson et al. 2016](#); [Hall et al. 2016](#)). HARPS3 will be a close-copy to HARPS ([Mayor et al. 2003](#); [Rupprecht et al. 2004](#)) and HARPS-North ([Cosentino et al. 2012](#)). The Terra Hunting Experiment (THE) will be conducted on HARPS3. THE aims to discover Earth-twins via 10-years of daily observations of at least 40 bright nearby Sun-like stars. By combining the high precision of HARPS3 with the radical observation plan of THE, observers have the greatest chance at detecting low mass, long period exoplanets. In fact, it has been shown that THE can detect Earth-twins in the habitable zone of Solar-type stars, for both single and multi-planet systems and with stellar signals ([Hall et al. 2018](#)). Further,

simulations have suggested that THE can outperform a typical reference survey and performs comparably to an uninterrupted space-based schedule on accuracy of recovered parameters for Earth-twin detection (Hall et al. 2018).

2.3. *Gaia*

Gaia is a space-based telescope with the mission to chart a three-dimensional map of the Milky Way, in pursuit of understanding the formation, composition, and evolution of the Milky Way. *Gaia*, which launched in 2013, had a nominal mission length of 5 years, but it has been extended through 2022 with an possible extension through 2025. *Gaia* will release astrometric observation in an upcoming data release, and is expected to have a significant impact on the knowledge of both exoplanet demographics and physical properties. The utility of *Gaia* for exoplanet detection and characterization via the astrometric method has been well studied, and current models and simulations predict the detection of $\sim 21,000$ exoplanets for a 5 year mission (Bernstein & Bastian 1995; Casertano et al. 1996; Casertano et al. 2008; Perryman et al. 2014; Ranalli et al. 2018). By combining astrometric data from *Gaia* and *Roman* we can extend the baseline of observations, thus extending sensitivity to period up to and potentially beyond 10 years.

It would be good to add a bit more of a project overview before you start describing technical details. Describe what kinds of planetary systems you'll simulate and why this will help answer the question.

I suggest making a new section called methods which starts with an overview of what kind of planetary systems you're going to simulate, then introduces modeling methods with technical details. I would probably put the equations before the description of sampling methods: exoplanet and PyMC3.

3. METHODS

3.1. *exoplanet* Code

For both simulating the orbits of the planets sampled in our paper and efficiently modeling the subsequent orbits, we use the *exoplanet* codebase. *exoplanet* is an open source toolkit that uses efficient gradient based sampling to model exoplanet data from transits, radial velocities, and/or astrometry (Foreman-Mackey et al. 2021). Practically, in its gradient-based inference, *exoplanet* uses methods such as Hamiltonian Monte-Carlo (), No U-Turn Sampling (), and variational inference (), which can improve performance (especially when there are more than 10 parameters) by orders of magnitude vs. other modeling methods such as Markov-Chain Monte Carlo (MCMC) (Foreman-Mackey et al. 2021). In contrast to many other tools in the vast ecosystem of exoplanet and time domain modeling software, *exoplanet* is designed as a framework with which a pipeline can be generated – rather than a finished code base with a “push go” button (Foreman-Mackey et al. 2021). *exoplanet* uses PyMC3, a model building language and inference engine that scales well in the many parameter regime (Salvatier et al. 2016).

In brief, given a set of orbital parameters, a cadence of observations, a duration of observations, and assuming an error, we can create a simulated dataset of both radial velocity and astrometry observations for a single exoplanet. We then model this simulated data using *exoplanet* and determine whether these orbital parameters can be accurately recovered. See Figure 3.1 for a schematic of this process.

3.2. Simulating Earth and Jupiter analogues

Add to section about simulating data, will do so once more concrete on simulated planetary parameters. We use *exoplanet* to simulate both the theoretical radial velocity and astrometric signals. For the radial velocity data, we adopt THE’s nightly cadence and 10 year duration, as described in Hall et al. (2018) while for the astrometric simulated data, we chose a cadence and duration of observations. We then introduce random gaussian noise to both the radial velocity and astrometry signals – producing our simulated dataset.

3.3. Modeling Pipeline

3.3.1. Radial Velocity Model

We then sample the parameter space using gradient-based MCMC with *exoplanet* for the three simulated planetary populations (Earth-like only, Jupiter-like only, and Earth-like and Jupiter-like) around Solar mass and radius stars. We adopted the expected precision of the

Table 1. Parameters for the Radial Velocity MCMC Model

Parameter	Prior ^a	Starting Point
$\log P$	$\mathcal{N}(\log P_0, \sigma_{P_0}^2)$	$\log P_0$
$\log K$	$\mathcal{N}(\log K_0, 5^2)$	$\log K_0$
$\sqrt{e} \cos \omega$	$\mathcal{U}(0, 1)$	0.01
$\sqrt{e} \sin \omega$	$\mathcal{U}(0, 1)$	0.01
T_0	$\mathcal{N}(T_{0,0}, \sigma_{T_{0,0}}^2)$	$T_{0,0}$

^a Priors adopted in the MCMC model. $\mathcal{U}(x, y)$ denotes a uniform distribution between x and y . $\mathcal{N}(\mu, \sigma^2)$ denotes a Gaussian distribution centered at μ with a standard deviation of σ .

THE radial velocity and *Roman* astrometric observations, placing Gaussian uncertainties on the data points with the same standard deviation as the those used to simulate the data ($\sigma_{RV} = 0.01$ m/s, $\sigma_\rho = 0.001''$, $\sigma_\theta = 0.1$ rad). First, we fit a radial velocity only model, in order to initially sample the parameter space without mass-inclination determination. We sample period (P), eccentricity (e), argument of the periapsis of the star (ω), radial velocity semi-amplitude (K), and the time of transit (T_0). As is standard in MCMC modeling of exoplanet radial velocity data, we sampled the eccentricity and argument of periapsis as $\sqrt{e} \cos \omega$ and $\sqrt{e} \sin \omega$ (cite *exofast*, others?). Additionally, we sampled period and semi-amplitude in natural logarithmic space. The five radial velocity modeling parameters, priors, and starting points can be seen in Table 1.

In modeling the simulated data, we followed the standard Keplerian equations. Including the magnitude of barycentric motion of the star (γ), which we set to zero as it is just a constant, the radial velocity signal is described by:

$$RV(\nu) = K \left[\cos(\nu(t) + \omega) + e \cos \omega \right] + \gamma \quad (2)$$

where

$$K = \left(\frac{2\pi G}{P} \right)^{\frac{1}{3}} \frac{M_p \sin i}{m_*^{\frac{2}{3}}} \frac{1}{\sqrt{1 - e^2}} \quad (3)$$

I am confused by the treatment of true anomaly, mean anomaly, and eccentric anomaly as used by *exoplanet* and the exact process used to solve Kepler’s equations. In the paper, they mention “In practice, we have found it more efficient to fuse the calculations of the eccentric anomaly E and the true anomaly f working only with the sine and cosines of these quantities.” I need to look more into this and then complete this section

3.3.2. Radial Velocity and Astrometric Model

Now that we have a sense of the radial velocity parameter space, we can include the astrometric data and

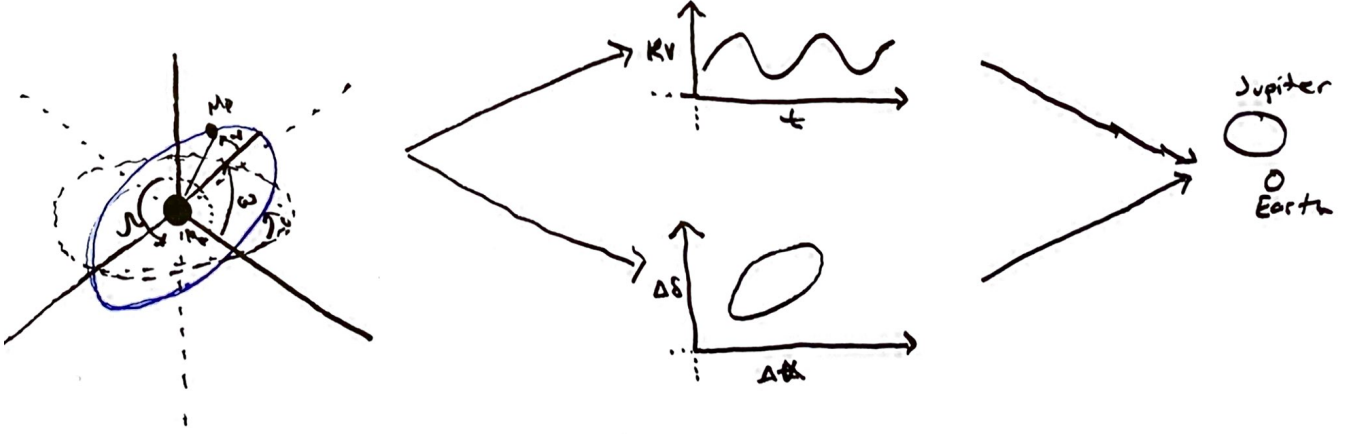


Figure 2. Schematic of process from orbital parameters, to simulated data, to final predictions.

Table 2. Parameters for the Joint Radial Velocity and Astrometric MCMC Model

Parameter	Prior ^a	Starting Point
$\log P$	$\mathcal{N}(\log P_{\text{RV}}, \sigma_{P_{\text{RV}}}^2)$	$\log P_{\text{RV}}$
$\log K$	$\mathcal{N}(\log K_{\text{RV}}, \sigma_{K_{\text{RV}}}^2)$	$\log K_{\text{RV}}$
$\sqrt{e} \cos \omega$	$\mathcal{U}(0, 1)$	$\sqrt{e} \cos \omega_{\text{RV}}$
$\sqrt{e} \sin \omega$	$\mathcal{U}(0, 1)$	$\sqrt{e} \sin \omega_{\text{RV}}$
T_0	$\mathcal{N}(T_{0,\text{RV}}, \sigma_{T_{0,\text{RV}}}^2)$	$T_{0,\text{RV}}$
m_p	$\mathcal{U}(0, 30) M_{\oplus}$...
i	$\mathcal{U}(0, \pi/2)$...
Ω	$\mathcal{U}(-\pi, \pi)$...

^a Priors adopted in the MCMC model. $\mathcal{U}(x, y)$ denotes a uniform distribution between x and y . $\mathcal{N}(\mu, \sigma^2)$ denotes a Gaussian distribution centered at μ with a standard deviation of σ .

model, and jointly sample radial velocity and astrometric parameter space using both simulated datasets in order to recover a complete posterior sample. As we are testing different astrometric observational cadences and durations, modeling the RV observations independently first has the added benefit of speeding up the astrometric modeling. By using the RV fit as a starting point for the joint MCMC, for all parameters besides the longitude of the ascending node (Ω) and splitting the mass-inclination degeneracy (m_p and i), we can more efficiently model the larger parameter space. We adopt the median parameters from the RV MCMC fit as the starting points in the joint fit MCMC and place Gaussian priors on three of the five orbital parameters (P , K , and T_0) with standard deviations equal to the RV MCMC standard deviations. The complete set of modeled parameters, priors, and starting points for the joint radial velocity and astrometric model can be seen in Table 2.

In modeling the astrometric data, we used the following astrometric equations, which are built into *exoplanet*. Including both parallax and proper motion, the total astrometric signal is described by

$$\xi(t) = \alpha_0^* + \pi_{\alpha^*} \pi + (t - t_0) \mu_{\alpha^*} + B X(t) + G Y(t) \quad (4)$$

$$\eta(t) = \delta_0 + \pi_{\delta} \pi + (t - t_0) \mu_{\delta} + A X(t) + F Y(t) \quad (5)$$

where α_* = $\alpha \cos \delta$, (α_0^*, δ_0) is the reference right ascension and declination of the star, ($\pi_{\alpha^*}, \pi_{\delta}$) is the parallax factors describing the parallactic ellipse of the star, and ($\mu_{\alpha^*}, \mu_{\delta}$) is the proper motion vector of the star. The equation above is parametrized by the Thiele-Innes constants (need to check whether omega values below are for the star or planet.)

$$A = \theta(\cos \Omega \cos \omega - \sin \Omega \sin \omega \cos i) \quad (6)$$

$$B = \theta(\sin \Omega \cos \omega + \cos \Omega \sin \omega \cos i) \quad (7)$$

$$F = \theta(-\cos \Omega \sin \omega - \sin \Omega \cos \omega \cos i) \quad (8)$$

$$G = \theta(-\sin \Omega \sin \omega + \cos \Omega \cos \omega \cos i) \quad (9)$$

where θ is the semi-major axis of the apparent ellipse or what we will call the astrometric signal due to an orbiting planet. The semi-major axis of the apparent ellipse can be solved using Kepler's Third Law (where m_{tot} is the total mass, or for a single planet system $m_{\text{tot}} = m_* + m_p$):

$$\theta = \left[\frac{P^2 G m_{\text{tot}}}{4\pi^2} \right]^{\frac{1}{3}} \quad (10)$$

If we assume a circular orbit and that $m_p \ll m_*$. At a distance “ d ” = $\frac{1}{\pi}$) from the observer and an orbital radius “ R ” = a , the astrometric signal equals...

$$\theta = \frac{m_p}{m_\star} \frac{R}{d} = \left(\frac{G}{4\pi^2} \right)^{1/3} \frac{m_p}{m_\star^{2/3}} \frac{P^{2/3}}{d} \quad (11)$$

$$\theta = 3 \mu\text{as} \cdot \left(\frac{m_p}{M_\oplus} \right) \left(\frac{m_\star}{M_\odot} \right)^{-2/3} \left(\frac{P}{\text{yr}} \right)^{2/3} \left(\frac{d}{\text{pc}} \right)^{-1} \quad (12)$$

Lastly, $(X(t), Y(t))$ is the vector describing the motion of the star caused by its planetary orbit. The vector is defined by

$$X(t) = \cos(E(t)) - e \quad (13)$$

$$Y(t) = \sqrt{1 - e^2} \sin(E(t)) \quad (14)$$

where E is the eccentric anomaly

$$E = M + e \sin E \quad (15)$$

and M is the mean anomaly, which can be determined by a series expansion of the true anomaly and the eccentricity (?)

add series expansion for M .

3.4. Synergies of Astrometric and Radial Velocity Equations

Add derivation of synergistic period dependence of astrometry and RV signals

Facilities:

Software:

APPENDIX

A. APPENDIX INFORMATION

REFERENCES

- Batygin, K., & Laughlin, G. 2015, Proceedings of the National Academy of Science, 112, 4214, doi: [10.1073/pnas.1423252112](https://doi.org/10.1073/pnas.1423252112)
- Bernstein, H. H., & Bastian, U. 1995, in ESA Special Publication, Vol. 379, Future Possibilities for Astrometry in Space, ed. M. A. C. Perryman & F. van Leeuwen, 55
- Casertano, S., Lattanzi, M. G., Perryman, M. A. C., & Spagna, A. 1996, Astrophysics and Space Science, 241, 89, doi: [10.1007/BF00644218](https://doi.org/10.1007/BF00644218)
- Casertano, S., Lattanzi, M. G., Sozzetti, A., et al. 2008, A&A, 482, 699, doi: [10.1051/0004-6361/20078997](https://doi.org/10.1051/0004-6361/20078997)
- Correia, A. C. M., Udry, S., Mayor, M., et al. 2005, A&A, 440, 751, doi: [10.1051/0004-6361/20042376](https://doi.org/10.1051/0004-6361/20042376)
- Cosentino, R., Lovis, C., Pepe, F., et al. 2012, in Society of Photo-Optical Instrumentation Engineers (SPIE) Conference Series, Vol. 8446, Ground-based and Airborne Instrumentation for Astronomy IV, ed. I. S. McLean, S. K. Ramsay, & H. Takami, 84461V, doi: [10.1117/12.925738](https://doi.org/10.1117/12.925738)
- Cumming, A., Butler, R. P., Marcy, G. W., et al. 2008, PASP, 120, 531, doi: [10.1086/588487](https://doi.org/10.1086/588487)
- Foreman-Mackey, D., Savel, A., Luger, R., et al. 2021, exoplanet-dev/exoplanet v0.4.5, doi: [10.5281/zenodo.1998447](https://doi.org/10.5281/zenodo.1998447)
- Gaia Collaboration, Prusti, T., de Bruijne, J. H. J., et al. 2016, A&A, 595, A1, doi: [10.1051/0004-6361/201629272](https://doi.org/10.1051/0004-6361/201629272)
- Gomes, R., Levison, H. F., Tsiganis, K., & Morbidelli, A. 2005, Nature, 435, 466, doi: [10.1038/nature03676](https://doi.org/10.1038/nature03676)
- Hall, R. D., Thompson, S., & Queloz, D. 2016, in Society of Photo-Optical Instrumentation Engineers (SPIE) Conference Series, Vol. 9915, High Energy, Optical, and Infrared Detectors for Astronomy VII, ed. A. D. Holland & J. Beletic, 991525, doi: [10.1117/12.2232487](https://doi.org/10.1117/12.2232487)
- Hall, R. D., Thompson, S. J., Handley, W., & Queloz, D. 2018, MNRAS, 479, 2968, doi: [10.1093/mnras/sty1464](https://doi.org/10.1093/mnras/sty1464)
- Johnson, S. A., Penny, M., Gaudi, B. S., et al. 2020, AJ, 160, 123, doi: [10.3847/1538-3881/aba75b](https://doi.org/10.3847/1538-3881/aba75b)
- Knutson, H. A., Fulton, B. J., Montet, B. T., et al. 2014, ApJ, 785, 126, doi: [10.1088/0004-637X/785/2/126](https://doi.org/10.1088/0004-637X/785/2/126)
- Latham, D. W., Mazeh, T., Stefanik, R. P., Mayor, M., & Burki, G. 1989, Nature, 339, 38, doi: [10.1038/339038a0](https://doi.org/10.1038/339038a0)
- Masuda, K., Winn, J. N., & Kawahara, H. 2020, AJ, 159, 38, doi: [10.3847/1538-3881/ab5c1d](https://doi.org/10.3847/1538-3881/ab5c1d)
- Mayor, M., & Queloz, D. 1995, Nature, 378, 355, doi: [10.1038/378355a0](https://doi.org/10.1038/378355a0)
- Mayor, M., Pepe, F., Queloz, D., et al. 2003, The Messenger, 114, 20
- Melchior, P., Spergel, D., & Lanz, A. 2018, AJ, 155, 102, doi: [10.3847/1538-3881/aaa422](https://doi.org/10.3847/1538-3881/aaa422)
- Morbidelli, A., Levison, H. F., Tsiganis, K., & Gomes, R. 2005, Nature, 435, 462, doi: [10.1038/nature03540](https://doi.org/10.1038/nature03540)
- Penny, M. T., Gaudi, B. S., Kerins, E., et al. 2019, ApJS, 241, 3, doi: [10.3847/1538-4365/aafb69](https://doi.org/10.3847/1538-4365/aafb69)

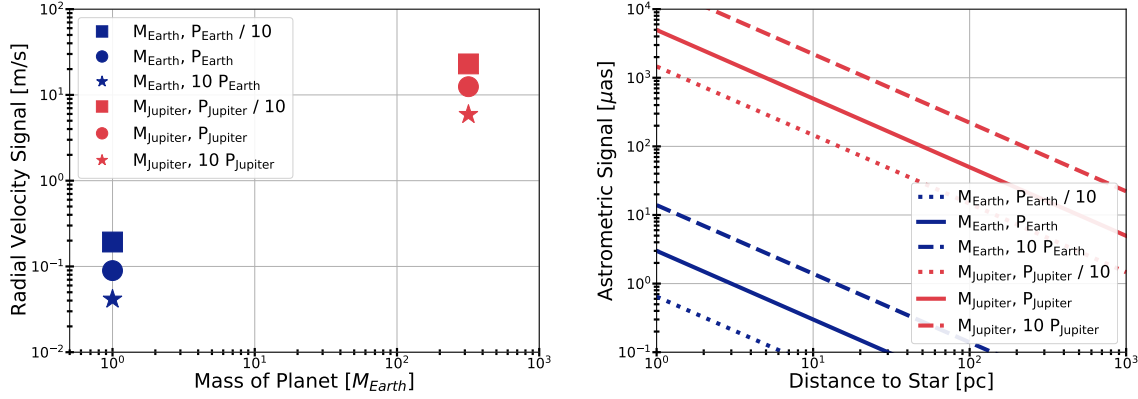


Figure 3. Radial velocity and astrometric signal for Earth-mass and Jupiter mass objects with periods of 0.1x, 1x, and 10x their solar-system values. RV signal for Earth-mass and Jupiter-mass objects on circular orbits around a Solar mass star. THE is pushing towards 0.1 m/s. (Right) Astrometric signal for Earth-mass and Jupiter-mass objects around Solar mass stars with varying period. Roman astrometry is pushing towards $\sim 1\text{--}10 \mu\text{as}$.

Perryman, M., Hartman, J., Bakos, G. Á., & Lindegren, L. 2014, *ApJ*, 797, 14, doi: [10.1088/0004-637X/797/1/14](https://doi.org/10.1088/0004-637X/797/1/14)

Ranalli, P., Hobbs, D., & Lindegren, L. 2018, *A&A*, 614, A30, doi: [10.1051/0004-6361/201730921](https://doi.org/10.1051/0004-6361/201730921)

Raymond, S. N., Quinn, T., & Lunine, J. I. 2004, *Icarus*, 168, 1, doi: [10.1016/j.icarus.2003.11.019](https://doi.org/10.1016/j.icarus.2003.11.019)

Riess, A. G., Casertano, S., Anderson, J., MacKenty, J., & Filippenko, A. V. 2014, *ApJ*, 785, 161, doi: [10.1088/0004-637X/785/2/161](https://doi.org/10.1088/0004-637X/785/2/161)

Rupprecht, G., Pepe, F., Mayor, M., et al. 2004, in *Society of Photo-Optical Instrumentation Engineers (SPIE) Conference Series*, Vol. 5492, Ground-based Instrumentation for Astronomy, ed. A. F. M. Moorwood & M. Iye, 148–159, doi: [10.1117/12.551267](https://doi.org/10.1117/12.551267)

Salvatier, J., Wiecki, T. V., & Fonnesbeck, C. 2016, *PeerJ Computer Science*, 2, e55

Spergel, D., Gehrels, N., Baltay, C., et al. 2015, *arXiv e-prints*, arXiv:1503.03757. <https://arxiv.org/abs/1503.03757>

Thompson, S. J., Queloz, D., Baraffe, I., et al. 2016, in *Society of Photo-Optical Instrumentation Engineers (SPIE) Conference Series*, Vol. 9908, Ground-based and Airborne Instrumentation for Astronomy VI, ed. C. J. Evans, L. Simard, & H. Takami, 99086F, doi: [10.1117/12.2232111](https://doi.org/10.1117/12.2232111)

Tsiganis, K., Gomes, R., Morbidelli, A., & Levison, H. F. 2005, *Nature*, 435, 459, doi: [10.1038/nature03539](https://doi.org/10.1038/nature03539)

Walsh, K. J., Morbidelli, A., Raymond, S. N., O’Brien, D. P., & Mandell, A. M. 2011, *Nature*, 475, 206, doi: [10.1038/nature10201](https://doi.org/10.1038/nature10201)

WFIRST Astrometry Working Group, Sanderson, R. E., Bellini, A., et al. 2019, *Journal of Astronomical Telescopes, Instruments, and Systems*, 5, 044005, doi: [10.1117/1.JATIS.5.4.044005](https://doi.org/10.1117/1.JATIS.5.4.044005)

Wolszczan, A., & Frail, D. A. 1992, *Nature*, 355, 145, doi: [10.1038/355145a0](https://doi.org/10.1038/355145a0)

Zhu, W., & Wu, Y. 2018, *AJ*, 156, 92, doi: [10.3847/1538-3881/aad22a](https://doi.org/10.3847/1538-3881/aad22a)